

Open Vocabulary Multi-Label Classification with Dual-Modal Decoder on Aligned Visual-Textual Features

Shichao Xu
Northwestern University
Evanston, USA

shichaoxu2023@u.northwestern.edu

Yikang Li
OPPO US Research Center
Palo Alto, USA

yikang.lil@oppo.com

Jenhao Hsiao
OPPO US Research Center
Palo Alto, USA

mark@oppo.com

Chiuman Ho
OPPO US Research Center
Palo Alto, USA

chiuman@oppo.com

Zhu Qi
Northwestern University
Evanston, USA

qzhu@northwestern.edu

Abstract

In computer vision, multi-label recognition are important tasks with many real-world applications, but classifying previously unseen labels remains a significant challenge. In this paper, we propose a novel algorithm, Aligned Dual-modal Classifier (ADDS), which includes a Dual-Modal decoder (DM-decoder) with alignment between visual and textual features, for open-vocabulary multi-label classification tasks. Then we design a simple and yet effective method called Pyramid-Forwarding to enhance the performance for inputs with high resolutions. Moreover, the Selective Language Supervision is applied to further enhance the model performance. Extensive experiments conducted on several standard benchmarks, NUS-WIDE, ImageNet-1k, ImageNet-21k, and MS-COCO, demonstrate that our approach significantly outperforms previous methods and provides state-of-the-art performance for open-vocabulary multi-label classification, conventional multi-label classification and an extreme case called single-to-multi label classification where models trained on single-label datasets (ImageNet-1k, ImageNet-21k) are tested on multi-label ones (MS-COCO and NUS-WIDE).

1. Introduction

Image classification tasks are fundamental and critical in computer vision. In recent years, with the advancement of deep neural networks, image classification has made a great impact in many real-world applications, such as medical imaging [28], autonomous driving [11], manufacturing [39], agriculture [19], etc. The most prevalent and well-studied topic in image classification is the *single-label*

classification [8, 40], which assumes that each image contains only one item, scene, or concept of interest to be labeled. Then, the topic of conventional *multi-label classification* [44, 43, 12] is brought out to address the case where multiple objects, scenes, or concepts in the same image are of interest and need to be labeled.

However, the conventional multi-label classification still cannot meet the need of some real-world applications where unseen labels may occur during testing. Previously, the task with unseen labels is often referred to as multi-label zero-shot learning. The related methods are often created based on label correlations [24, 32], which try to identify potential relations among the labels within the image to facilitate classification, usually, through building a label graph. Moreover, some methods [3, 30], including the previous state-of-the-art (SOTA) method ML-Decoder [41], create label embeddings solely from the words or assign learnable embeddings for each label instead of indirectly creating and learning from the graph relation, allowing for more sophisticated outcomes. One of the mostly used label embeddings is Word2Vec [34], which is created from pretraining tasks with external textual datasets (target label classes can be seen during pre-training). Then by extracting local discriminative features according to different label embeddings, the model outputs the per-class probability. However, these models only focus on the connection between the words, and the generalization of the learned mapping (from image to seen label) to the target mapping (from image to unseen label) is still challenging. The leveraging of the word embedding also blocks the model from handling phase/sentence labels, which also exist in practice and are very challenging to address.

In [48], the *Open-Vocabulary* setting is introduced,

which is a generalization of zero-shot and weakly supervised settings and is more suitable for dealing with unseen classes. While the target classes are not known during training, it can be any subset of the entire language vocabulary in the pretraining tasks (e.g., contrastive learning on image-caption dataset). It is proved to be quite effective in some computer vision tasks, such as object detection [10] and object segmentation [14]. In this setting, instead of using costly annotations for classification datasets, the Vision-Language Pretraining (VLP) model trained on image-caption datasets can be utilized to help build the connection between the visual and textual embeddings and provide more flexibility in algorithm design.

However, current VLP models are not silver bullets and present new challenges. Practical VLP models are usually trained with fixed low-resolution images for reducing the computational cost of large-scale data sources. The input resolution for the model adapted from those VLP models will be restricted. Besides, identifying whether a label exists in the image from their embeddings is also challenging, as the measurement based on simply comparing the cosine similarity can lead to an uncertain threshold (which is typically different for different images and objects.) Besides, given the difficulty and cost to collect and annotate multi-label datasets, we also consider a somewhat extreme but practically useful setting where models trained on single-label datasets (e.g., ImageNet-1k) are tested on multi-label datasets with unseen categories (e.g., NUS-WIDE). We call this *single-to-multi label classification*.

In this work, we develop a novel approach for open-vocabulary multi-label classification that significantly outperforms previous methods and provides the new state-of-the-art (SOTA) performance. In three classification tasks – open-vocabulary multi-label, single-to-multi label, and conventional multi-label – our approach provides significantly higher mean Average Precision (mAP) than previous methods, including SSGRL [5], MS-CMA [47], ASL [2], Q2L [30], LESA [18], BiAM [36], GMLZSL [17], SDL [3], ML-Decoder [41]. More specifically, to overcome the challenges in previous methods, we propose an open-vocabulary multi-label classification framework **ADDS** (Aligned Dual modality ClaSsifier) based on the aligned visual and textual embeddings. The framework includes a novel **DM-decoder** (Dual-Modal decoder) design, which leverages the dual modality to enhance transformer decoder layers by progressively fusing visual embeddings with textual information and developing richer semantic understanding. It also includes a **Pyramid-Forwarding** method to adapt the model pre-trained on lower image resolutions to higher resolution images without re-training. To summarize, our work makes the following technical contributions:

- We have developed ADDS, an open-vocabulary multi-label classification framework that builds on aligned

visual and textual features. The framework includes DM-Decoder, a novel transformer decoder for facilitating the fusion of the semantics from dual-modal information source, and Pyramid-Forwarding, a new adaptation method that addresses images with higher resolutions than training images and is also able to largely reduce the computational cost of vision transformer.

- We have conducted extensive experiments across various multi-label classification tasks. Our ADDS framework significantly outperforms the previous SOTA methods in all scenarios, including open-vocabulary multi-label classification (11.57 points improvement on NUS-WIDE), single-to-multi label classification (24.71 points and 16.49 points improvements from ImageNet-1k to MS-COCO and NUS-WIDE, respectively), and conventional multi-label classification (e.g., 2.14 points improvement on MS-COCO).

2. Related Works

2.1. Conventional Multi-label Classification

Conventional multi-label classification, which aims to classify multiple objects, scenes, or concepts in a given image, is generally a more challenging task than the typical single-label classification. It has been studied in the literature by various approaches. The first group of methods is based on the region of interest. And in previous works such as [44, 43, 12, 47, 12], multi-label classification is solved by locating each object in the image or capturing the attention map and then performing single-label classification on it. However, these methods often suffer from issues like coarse discovered regions, heavy computation costs, some concepts or scenes being hard to localize, and some regions containing duplicate concepts. Another group of methods is based on label correlations. They try to identify the potential relations among the labels within the training images to facilitate classification [5, 42, 46]. For instance, the method in [5] splits the feature representation into category semantics-specific representations and applies a graph neural network to explore the interactions among them. Some previous multi-label zero-shot learning methods also share a similar idea with conventional multi-label classification, which will be discussed in the next section.

2.2. Multi-Label Zero-Shot Classification

Some of the methods for conventional multi-label classification claim that they can also address zero-shot classification, such as [44, 41]. There are also other previous works [37, 1, 49, 20, 18, 36]. Generally speaking, many papers in recent years try to capture the unseen labels by exploring the connections between the labels. For instance, Akata et al. [1] consider each class as an embedding in

the space of attribute vectors, and then introduce a function measuring the compatibility between an image and a label embedding to determine the correct classes. The work in [49] studies the image-word relevance by estimating the principal direction for an image, which is based on the assumption that the word vectors of relevant labels for a given image can rank ahead of the irrelevant labels along a principal direction in the word vector space. The most recent paper in multi-label zero-shot learning is [41], which employs Word2Vec to generate the label text embedding and solely relies on the relation between the text features for learning. However, due to a lack of supervision on the visual information during the textual embedding learning, the learned mapping between the image and text is hard to be generalized to unseen data space.

2.3. Vision-Language Pre-training (VLP)

The vision language pre-training learns the semantic correspondence between image and language by pretraining on large-scale data with different tasks. In the literature, some works such as VisualBERT [27], Unicoder-VL [25], and ViLT [21] extract image tokens from the interest regions, combine them with language tokens together as the inputs, and fuse the information by the transformer in the early stage. Other works such as Contrastive Language-Image Pre-training (CLIP) [38], Self-supervision meets Language-Image Pre-training (SLIP) [35], Bootstrapping Language-Image Pre-training (BLIP) [26], and Triple Contrastive Learning (TCL) [45] first extract the deep features of the image and the text individually, and then conduct modality interaction after the feature extraction. In this paper, we mainly maintain the alignment of the visual and textual embeddings through CLIP [38], which is built on the cosine similarity between the image and text embedding pairs and trained with a large and noisy dataset. Moreover, later in Section 4.4, we also introduce experiments on using other VLP models such as BLIP [26] and SLIP [35].

2.4. Open-Vocabulary Learning

VLP models enable a strong connection between images and corresponding textual information by learning from large-scale training corpora. Incorporating VLP models into model design has made arbitrary text label prediction possible, and numerous related applications have benefited from it. In recent years, open-vocabulary object detection [48, 13, 16, 4, 23] and open-vocabulary semantic segmentation [14, 33, 15] have become increasingly popular. Zareian et al. [48] firstly propose Open-Vocabulary object Detection (OVD) and connect it with image-text pre-training. Gao et al. [13] leverage the localization ability of the VLP model to generate pseudo bounding-box labels for training the open-vocabulary object detector. Besides, Gu et al. [16] further distill the knowledge from a

VLP model into a two-stage open-vocabulary object detector. When VLP models are leveraged for visual-semantic alignments on pixel-level information, Ma et al. [14] are able to make the zero-shot transfer to segment novel categories. In this paper, we utilize the CLIP model to keep the visual-semantic alignments to achieve open vocabulary multi-label classification.

3. Methodology

3.1. Overview

In this section, we present the details of our ADDS method for multi-label classification. As shown in Figure 1, our method receives both the image $x_{img} \in \mathbb{R}^{H \times W \times 3}$ and the class names $X_{lbl} \subset \{\text{natural language words}\}$ as the inputs, where X_{lbl} contain words of potential labels for identifying the objects (tree, apple, computer, ...), scenes (sea, sky, underground, ...) or concepts (small, red, ...). Then the classes names X_{lbl} are combined with prompts such as "This photo contains @" and "This is a @ photo", where $@ \in X_{lbl}$, and fed through a text tower to get the textual (class) embedding. The image input is fed through the Pyramid-Forwarding module, whose output images are then fed through an image tower to get the visual (image) embedding. The visual embedding is aligned with textual embedding, and then stacked and forwarded to the DM-decoder, whose outputs are mapped to per-class probabilities via a shared fully-connected layer. That is, given the input $\{x_{img}, X_{lbl}\}$, our model outputs $p_{pred} = [p_1, p_2, \dots, p_k]$, where $p_i \in [0, 1]$, $k = |X_{lbl}|$.

Compared with previous works [30, 41] where the label embedding is learned from limited observations, or based on Word2Vec [41] or even randomly initialized matrix [41], a major difference of our approach is that our model is constructed based on the alignment between visual and textual embeddings. This is not only helpful for conventional multi-label classification, but also critical for boosting the performance of open-vocabulary multi-label classification. Specifically, in our setting, the training data contains the images $\{x_{(img, seen)}\}$ and the labels $X_{(lbl, seen)}$. The objective is to learn a classifier g to make predictions on an unseen image $x_{(img, unseen)}$ with unseen categories $X_{(lbl, unseen)}$, i.e., $g(x_{(img, unseen)}, x_{(lbl, unseen)}) \in \{0, 1\}$, $g() = 1$ if $x_{(img, unseen)}$ contains object/scene/concept $x_{(lbl, unseen)}$, and $g() = 0$ otherwise. Inspired by VLP, we build the visual-semantic alignment with the help of the pre-trained model from CLIP. Specifically, we employ the vision transformer (ViT) [9] network architecture as the image encoder f_{img} and the multi-layer transformer as the text encoder f_{lbl} , with the parameters of both encoders from CLIP. They are all frozen during training to maintain the alignment (may lead to worse results if unfreeze). Next, we will introduce the major components in our ADDS method in details.

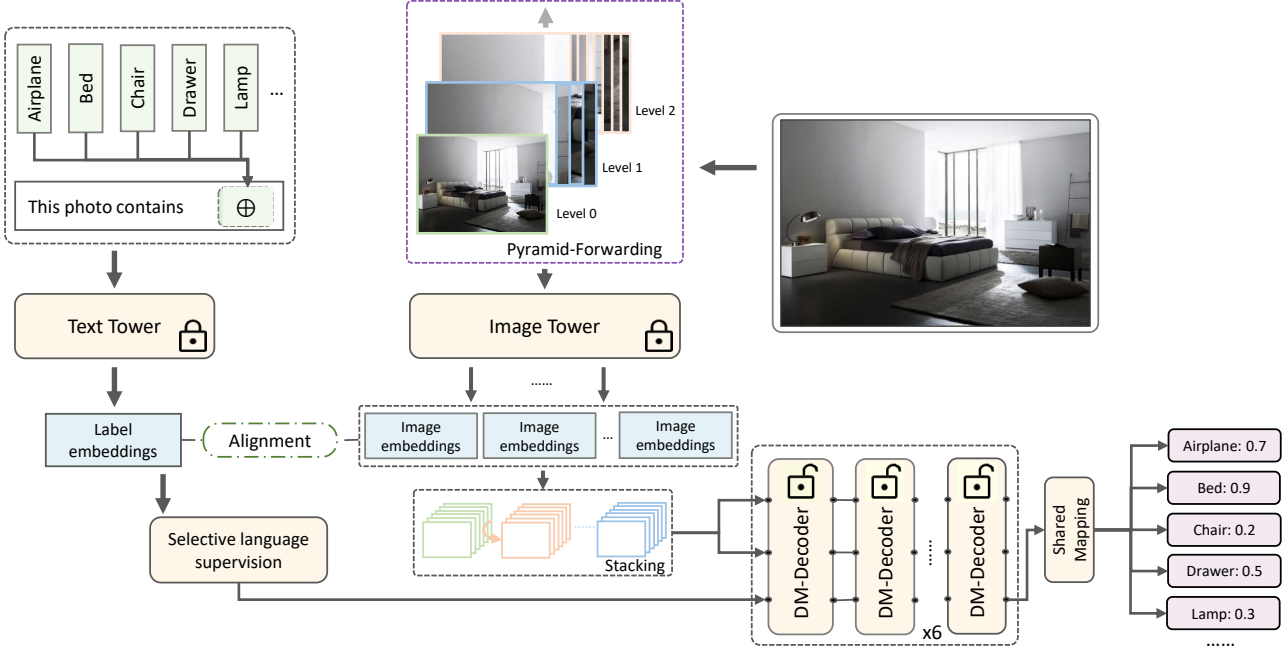


Figure 1. Overview of our ADDS framework for multi-label classification. Text labels with prompts are fed into a text tower to get the textual embedding. Images are first processed by a Pyramid-Forwarding module and then fed into an image tower to get the visual embeddings, which are aligned with the textual embedding and stacked on the token size dimension. Then the textual embedding (after a selective language supervision module) and the stacked visual embeddings are fused by six layers of DM-decoders with the initial query from textual embedding and the initial key/value from visual embeddings. After a shared mapping among all labels, the network outputs the probability for each label class.

3.2. Dual-Modal Decoder

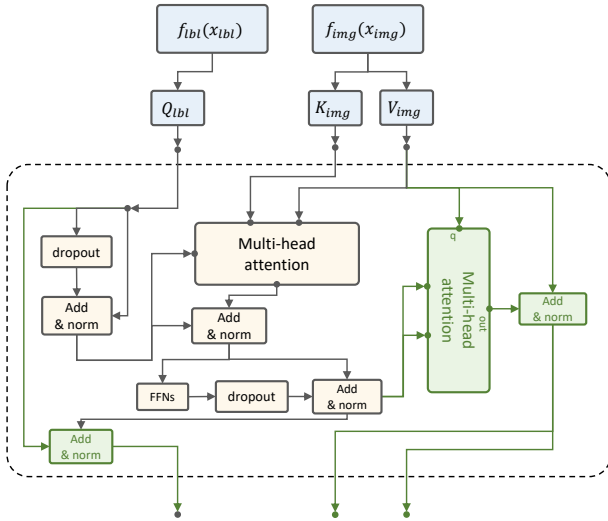


Figure 2. Overview of our Dual-Modal Decoder design.

The typical practice of aligned visual and textual embeddings in multi-label classification is to measure their cosine similarity. Given the visual embedding E_{img} from an image and a textual embedding E_{lbl} from a specific label, whether this image contains the label is determined by the calculated similarity score $s = \cos(\frac{E_{img}}{|E_{img}|}, \frac{E_{lbl}}{|E_{lbl}|})$ and a threshold η .

Usually, the image is deemed to contain the label if $s > \eta$.

In practice, η can be different when considering different images and labels, which presents a significant challenge. Inspired by ML-Decoder [41], this challenge can be mitigated by turning into a binary classification task with adding decoder layers. After the visual and textual feature extraction steps, a single layer cross-attention (we omit the description of the fully-connected layer, dropout, and layer normalization for space reason) is the choice for querying the textual embedding from the visual embedding to determine the per-class probability. However, we observe some issues when we stack decoder layers similarly as in [41]:

- The model performance will often decrease after stacking more than 3 decoder layers.
- The key and value inputs are always the same from the visual embedding. As the output of the cross-attention layer is a weighted sum of its value input, the outputs of decoder layers in different levels are actually in the same (or close) semantic level and all from the same visual embedding.

To address these issues, we redesign the decoder module, with two major differences from the previous method in [41], as shown in Figure 2 and Equation (1). Specifically, we add an additional multi-head cross-attention layer MultiHdAttn_2 and use the visual embedding V_{img} to query

the output Q_{mid}^5 from the previous cross-attention layer MultiHdAttn_1 , instead of using the textual embedding as the query (MultiHdAttn_1 utilizes the textual embedding to query the visual features). The output Q_{mid}^5 contains the weighted sum of image tokens' embedding guided by the textual information, so we can redistribute them back to each image tokens' embedding through MultiHdAttn_2 , to further enhance the visual embedding according to the correlation of Q_{mid}^5 with the key inputs. Then after adding and normalization, the key and value input for the next decoder layer are refined by the textual information. Moreover, apart from the original skipping structures, we add an additional skipping connection from the query input to the query output, which is transformed by addition and normalization.

Formally, we denote the input query, key, value as $Q_{lbl}, K_{img}, V_{img}$, and the block's output query, key and value for the next block as $Q'_{lbl}, K'_{img}, V'_{img}$. We output Q'_{lbl} only if it is the last layer. We denote DP as the dropout layer, and $\text{FFN}_1, \text{FFN}_2$ as the fully-connected layer. Then, each new decoder block can be formulated as:

$$\begin{aligned}
 Q_{mid}^1 &= \text{LayerNorm}(Q_{lbl} + \text{DP}(Q_{lbl})), \\
 Q_{mid}^2 &= \text{MultiHdAttn}_1(Q_{mid}^1, K_{img}, V_{img}), \\
 Q_{mid}^3 &= \text{LayerNorm}(Q_{mid}^2 + Q_{mid}^1), \\
 Q_{mid}^4 &= \text{DP}(\text{FFN}_1(\text{ReLU}(\text{FFN}_2(Q_{mid}^3))))), \\
 Q_{mid}^5 &= \text{LayerNorm}(Q_{mid}^4 + Q_{mid}^3), \\
 Q_{lbl} &= \text{LayerNorm}(Q_{mid}^5 + Q_{lbl}), \\
 V_{img}^1 &= \text{MultiHdAttn}_2(V_{img}, Q_{mid}^5, Q_{mid}^5), \\
 V'_{img} &= \text{LayerNorm}(V_{img}^1 + V_{img}), \\
 K'_{img} &= V'_{img}.
 \end{aligned} \tag{1}$$

3.3. Pyramid-Forwarding

A major challenge for using pre-trained models learned from large-scale datasets (e.g., the VLP models) is that they are often trained on low-resolution images (e.g., 224x224 or 336x336) due to the limitation of computational resources (training time, memory usage, etc.). Thus the extracted features are often not compatible with higher-resolution images. We could consider downsampling the higher-resolution input images to lower resolution, but that will lose significant local features. Conducting fine-tuning on higher-resolution images might slightly reduce the incompatibility with extracted features, but we still face several challenging questions: 1) Does the model support training on arbitrary scale images? 2) How much fine-tuning data are available to maintain the model's generalization ability? 3) How long or how well the model should be trained to avoid overfitting on the fine-tuning dataset?

To address these challenges, we propose Pyramid-Forwarding, a resolution-compatible method that enables deploying a pre-trained model trained from low-resolution images on high-resolution images without retraining. This method applies to many pre-trained image decoders, and

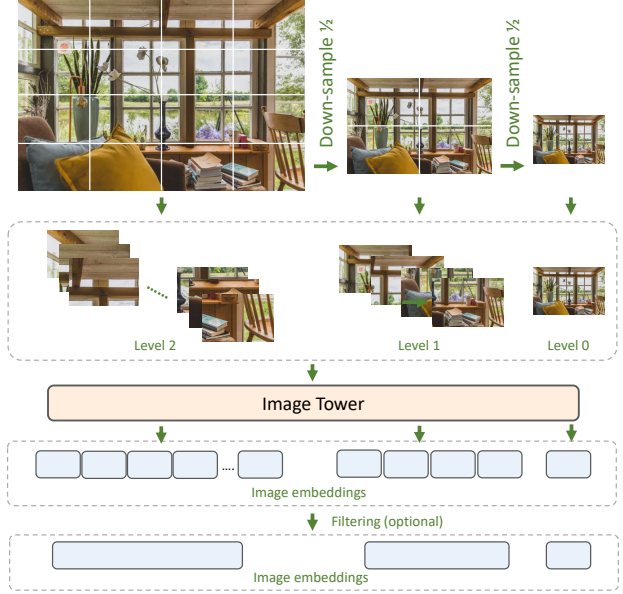


Figure 3. Overview of the Pyramid-Forwarding method.

below we use the ViT [9] pre-trained on $S_{Img} \times S_{Img}$ resolution images as an example. It will be applied on $S_{Img} * d \times S_{Img} * d$ target images (d is a positive integer), and our method helps reduce the computation cost from $O(d^4 \cdot c)$ to $O(d^2 \cdot c)$, where c is a constant for all resolutions.

Specifically, given a pre-trained model with $S_{Img} \times S_{Img}$ resolution and an image of size $S_{Img} * d \times S_{Img} * d$, Pyramid-Forwarding constructs $\log(d) + 1$ levels. First we assume that $\log(d)$ is an integer, and we will discuss the non-integer case later. In level $i \in [0 \dots \log(d)]$, the image is resized to $S_{Img} * 2^i \times S_{Img} * 2^i$ and split into $(i+1) \times (i+1)$ patches, as visualized in Figure 3. Then these patches are fed into the image encoder (usually wrapped into the batch dimension for parallel processing on GPUs) to obtain the feature tokens. In ViT, these tokens are stacked on the token dimension and then feed into the decoder, and the computation cost on the $S_{Img} * d \times S_{Img} * d$ image is actually $O((d^2)^2) = O(d^4)$ times more than the $S_{Img} \times S_{Img}$ image because of the self-attention layer. However, with Pyramid-Forwarding, this computation cost is reduced to $1 + 2^2 + 4^2 + \dots + (2^{\log(d)})^2 = O(d^2)$. If $\log(d)$ is not an integer, the size of the top-level image will be changed to S_{Img}^o , and we allow the divided patches to be overlapped with their neighborhoods, while the total number of patches in this level i is still $(i+1)^2$. In addition, the computation cost of Pyramid-Forwarding can be further reduced by disposing the image patches from the non-bottom levels $i \in [1 \dots \log(d)]$, which provides a trade-off between the accuracy and the computational cost. A special case that works well is when each non-bottom level only contains the

token embedding corresponding to the [CLS] token in ViT. It significantly reduces memory usage while moderately degrades the performance, when compared with the complete design.

3.4. Selective Language Supervision

As the label classes can be object/scene/concept names that are selected from the natural language, the total number of the labels can be extremely large (e.g., 1k in ImageNet-1k, 21k in ImageNet-21k, or even more). This presents a challenge in the training stage – if we feed all the labels into the network, it is a heavy burden on the inference speed and the memory usage. Thus we propose a *selective language supervision* method that utilizes the positive labels and part of the negative labels selected during the network training, and consider the data distribution of the positive and negative samples for reducing data imbalance.

Specifically, given multi-label $L = \{l_1, l_2, \dots, l_k\}$ from the training batch B with k classes in total, $S_{pos} = \{i | l_i = 1, l_i \in L, L \in B\}$, and $S_{neg} = \{1, 2, \dots, k\} - S_{pos}$. Then the selected label set for batch B training is

$$S' = S_{pos} \cup S_{slt}, \quad (2)$$

where elements in S_{slt} is randomly selected from S_{neg} . $|S_{slt}| = \min(\alpha * |S_{pos}|, k - |S_{pos}|)$, where α is a hyperparameter balancing the number of positive and negative samples (we choose $\alpha = 3$ in our experiments if not mentioned specifically). Note that the selective language supervision is only utilized in experiments with large label set (e.g., the ImageNet-21k dataset).

4. Experimental Results

4.1. Implementation Settings

Our code is implemented in PyTorch 1.10.2. All experiments are conducted on a server cluster running Ubuntu 18.04.6 and equipped with NVIDIA V100 GPUs. We conduct the experiments on NUS-WIDE [7], MS-COCO [29], ImageNet-1k [8], and ImageNet-21k [40] datasets. All models are optimized by the Adam optimizer [22]. The learning rate is set as 3×10^{-4} for all models trained on 224×224 and 336×336 images, and as 1×10^{-4} for all models trained on images larger than 336×336 . We test the input resolution of the images on 224×224 , 336×336 , 448×448 , 640×640 , 1344×1344 , and they are specified in each experiment. We adopt the ViT [9] as the image encoder and use CLIP [38] pre-trained weights. The output of ViT is $[bs, n_t, l]$, where $bs = 56$ is the batch size, n_t is the number of output tokens from the vision transformer, and l is the embedding length determined by the type of the vision transformer. All image and text towers in our method are fixed during the training. The model is trained for 40 epochs, and the weight decay is 10^{-4} . Our model applies

the loss function ASL from [2], which is also used in the most recent multi-label classification works [30, 41].

4.2. Open-Vocabulary Multi-label Classification

In open-vocabulary multi-label classification, we first show our results on the NUS-WIDE dataset in Table 1. The marking ‘uf’ means unfreezing the backbone network and ‘f’ means freezing the backbone network, and both markings are only used when ML-Decoder is switched to the same backbone as our model. To begin with, we use image-encoder ViT-B-32 and its corresponding text encoder with CLIP pre-trained weights. Using 224×224 input images, our ADDS method already achieves a 36.56% mAP, 5.46 points higher than the previous SOTA method ML-Decoder with TresNet-L as the backbone network architecture and trained on 448×448 input images. Then we use image-encoder ViT-L-336 and its corresponding text encoder with CLIP pre-trained weights on 336×336 images. The result further improves to a 39.01% mAP, 7.9 points higher than ML-Decoder (which uses higher resolution images than both of our first two settings). Finally, our result can reach 42.67% when trained on 448×448 images. We also show that when we use the same backbone network architecture ViT-L-336 and the same pretraining weights (with freezing or unfreezing the backbone) for ML-Decoder, our ADDS method still shows significant advantage (i.e., 39.01% mAP over 33.7% mAP for 336×336 images; note that ML-Decoder cannot be trained with 448×448 images for ViT-L-336 as it does not support input resolutions different from the original model resolution). Overall, the results in Table 1 clearly demonstrate that **our approach provides significant improvement over previous methods on open-vocabulary multi-label classification**.

Moreover, Table 2 shows the experimental results on the MSCOCO dataset. We make the data splitting in the following way: after sorting the class names in increasing alphabetical order, we select the first 65 classes to be the seen classes, and the rest 15 classes to be the unseen classes. The results show that our ADDS method can achieve much better results than the original ML-Decoder (59.18% vs. 30.69%), and when using the same backbone network, it still **significantly outperforms the ML-Decoder** (54.52% vs. 43.84%; note that ML-Decoder cannot take 448×448 images with ViT-L-336 as backbone).

4.3. Single-to-multi Label Classification

We compare our approach with the previous method ML-Decoder in an extreme case of open-vocabulary multi-label classification, where models are trained on the single-label ImageNet-1k dataset and tested on the multi-label MS-COCO and NUS-WIDE datasets. We show two cases, depending on whether the testing dataset contains the overlapped classes with ImageNet-1k or not. The results are

Method	Type	mAP(%)	F1 (k=3)	F1 (k=5)
CONSE	zsl	9.4	21.6	20.2
LabelEM	zsl	7.1	19.2	19.5
Fast0Tag	zsl	15.1	27.8	26.4
One Attention per Label	zsl	10.4	25.8	23.6
One Attention per Cluster (M=10)	zsl	12.9	24.6	22.9
LESA	zsl	19.4	31.6	28.7
BiAM	zsl	26.3	33.1	30.7
Generative ML-ZSL	zsl	25.7	32.8	29.3
SDL	zsl	25.9	30.5	27.8
ML-Decoder (TresNet-L, 448x448)	zsl	31.1	34.1	30.8
ML-Decoder (ViT-L-336, uf, 336x336)	zsl	16.6	16.2	17.8
ML-Decoder (ViT-L-336, f, 336x336)	zsl	33.7	31.0	32.1
ADDS (ViT-B-32, 224x224)	ov	36.56	34.22	36.65
ADDS (ViT-L-336, 336x336)	ov	39.01	36.96	39.28
ADDS (ViT-L-336, 448x448)	ov	42.67	38.27	40.49

Table 1. Comparison of different methods on open-vocabulary multi-label classification for the NUS-WIDE dataset. In the *Type* column, *zsl* means the zero-shot learning setting, *ov* means the open-vocabulary setting. Our ADDS method provides significantly better results than previous methods, including CONSE [37], LabelEM [1], Fast0Tag [49], One Attention per Label [20], One Attention per Cluster (M=10) [18], LESA [18], BiAM [36], Generative ML-ZSL [17], SDL [3], and ML-Decoder [41].

Method	Input Resolution	mAP(%)	F1(k=3)
ML-Decoder (ViT-L-336, f)	336x336	43.84	35.08
ML-Decoder (ViT-L-336, uf)	336x336	43.75	17.09
ML-Decoder (TresNet-L)	448x448	30.69	16.69
ADDS (ViT-L-336)	336x336	54.52	51.52
ADDS (ViT-L-336)	448x448	59.18	77.34

Table 2. Comparison on open-vocabulary multi-label classification for the MSCOCO dataset.

shown in Tables 3 and 4. Our approach greatly outperforms ML-Decoder, despite our model uses lower-resolution images (224×224 for ViT-B-32 backbone and 336×336 for ViT-L-336 backbone) than ML-Decoder (448×448). This again shows that **our approach greatly outperforms previous methods in single-to-multi label classification.**

4.4. Additional Experiments

4.4.1 Conventional Multi-label Classification

Apart from the open-vocabulary multi-label classification, we are also curious about how our model works on conventional multi-label classification. We conduct experiments

With overlapped classes				
Model	Backbone	mAP(%)	F1(k=3)	F1(k=5)
ML-Decoder	TResNet-L	41.60	17.80	17.80
ADDS	ViT-B-32	59.27	45.88	45.88
ADDS	ViT-L-336	67.10	50.86	50.86
Without overlapped classes				
Model	Backbone	mAP(%)	F1(k=3)	F1(k=5)
ML-Decoder	TResNet-L	38.37	6.90	6.90
ADDS	ViT-B-32	64.32	30.90	30.90
ADDS	ViT-L-336	69.60	33.16	33.16

Table 3. Comparison on single-to-multi label classification. Models are trained on ImageNet-1k and tested on MS-COCO. Our method greatly outperforms ML-Decoder.

With overlapped classes				
Model	Backbone	mAP(%)	F1(k=3)	F1(k=5)
ML-Decoder	TResNet-L	14.15	7.07	7.30
ADDS	ViT-B-32	27.34	20.39	20.39
ADDS	ViT-L-336	31.07	24.69	24.69
Without overlapped classes				
Model	Backbone	mAP(%)	F1(k=3)	F1(k=5)
ML-Decoder	TResNet-L	13.19	6.26	6.27
ADDS	ViT-B-32	26.96	16.07	16.07
ADDS	ViT-L-336	30.66	19.18	19.18

Table 4. Comparisons of single-to-multi label classification task which is trained on ImageNet-1k and tested on NUS-WIDE dataset. Our method shows the SOTA performance.

Model	Backbone	Input Resolution	mAP(%)
ML-GCN	ResNet101	448x448	83.0
KSSNET	ResNet101	448x448	83.7
SSGRL	ResNet101	576x576	83.8
MS-CMA	ResNet101	448x448	83.8
ASL	TResNet-L	448x448	88.4
Q2L	TResNet-L	448x448	89.2
ML-Decoder	TResNet-M	224x224	84.2
ML-Decoder	TResNet-L	448x448	90.1
ML-Decoder	TResNet-XL	640x640	91.4
ML-Decoder	ViT-L-336 (uf)	336x336	88.5
ML-Decoder	ViT-L-336 (f)	336x336	90.6
ADDS	ViT-L	224x224	89.82
ADDS	ViT-L-336	336x336	91.76
ADDS	ViT-L-336	640x640	93.41
ADDS	ViT-L-336	1344x1344	93.54

Table 5. Comparison on conventional multi-label classification for the MS-COCO dataset. Our ADDS approach shows significant improvement over previous methods, including ML-GCN [6], KSSNET [31], SSGRL [5], MS-CMA [47], ASL [2], Q2L [30], and ML-Decoder [41].

on the MS-COCO dataset, and the results are shown in Ta-

ble 5. We run a few variations of our approach and compare them with a number of baselines. We first use the ViT-L backbone [9] to test on 224×224 resolution images. We observe that our approach achieves an mAP of 89.82%, which is 5.6 points higher than the previous SOTA method ML-Decoder [41] on 224×224 images. We then switch to a larger image encoder ViT-L-336 for image resolution of 336×336 . Our approach achieves an mAP of 91.76%, which is even better than what ML-Decoder can achieve on higher-resolution images of 640×640 . And when we train our model with ViT-L-336 on 640×640 images, the mAP reaches 93.41%, 2.0 points higher than ML-Decoder at the same resolution. With Pyramid-Forwarding, our model can also be deployed efficiently on an even higher resolution of 1344×1344 with the model ViT-L-336 pre-trained on 336×336 resolution, and our approach can achieve an mAP of 93.54% (with much less computational cost than pre-training a model on 1344×1344 images).

4.4.2 Ablation Study: Effectiveness of DM-Decoder

We validate the effectiveness of our Dual-Modal decoder (DM-Decoder) design. In particular, we conduct the open-vocabulary multi-label classification experiments on NUS-WIDE. We replace the DM-Decoder in our approach with the decoder layer in the previous SOTA ML-Decoder under various number of stacking layers. The image resolution is 336×336 , and all image encoder is chosen as ViT-L-336. As shown in Table 6, DM-Decoder significantly outperforms the decoder design in ML-Decoder in almost all cases, showing its effectiveness.

Model	mAP(%)	F1 (k=3)	F1 (k=5)
ADDS+ML-Decoder \times 1	36.15	32.45	35.50
ADDS+ML-Decoder \times 3	36.35	31.33	34.89
ADDS+ML-Decoder \times 6	36.34	29.83	33.56
ADDS+DM-Decoder \times 1	36.88	32.95	35.48
ADDS+DM-Decoder \times 3	38.68	34.46	37.50
ADDS+DM-Decoder \times 6	39.01	36.96	39.28

Table 6. Comparison between DM-Decoder and ML-Decoder on NUS-WIDE for open-vocabulary multi-label classification.

4.4.3 Ablation Study: Full Pyramid-Forwarding vs. Single-layer Pyramid-Forwarding

We then evaluate the effectiveness of Pyramid-Forwarding by comparing the results of using only a single layer of Pyramid-Forwarding versus using full Pyramid-Forwarding on MS-COCO. We choose this dataset since it has higher resolution and more suitable for comparing on different resolutions. In Table 7, the second column shows the level index in Pyramid-Forwarding. The first line shows the result of using the model on 336×336 images without Pyramid-Forwarding. The second line shows the model with Pyramid-Forwarding on 1344×1344 images, but only

with the level of highest resolution (third level) and cutting into 16 patches. The third line shows the model with full Pyramid-Forwarding on 1344×1344 resolution images. We can see that using full Pyramid-Forwarding cannot provides much more performance boost.

Model	Level	Image Resolution	mAP(%)
ADDS	[0]	336x336	91.76
ADDS	[2]	1344x1344	91.79
ADDS	[0,1,2]	1344x1344	93.54

Table 7. Full vs. single-layer Pyramid-Forwarding.

4.4.4 Ablation Study: Impact of the Number of Training Classes

We claim that increasing the number of available training classes can benefit the single-to-multi label classification, and we validate this through training our model (on ViT-L-336) with the selective language supervision technique on the ImageNet-21k dataset. For a fair comparison, we filter out the overlapped classes with NUS-WIDE in ImageNet-1k, and we select the first 15k classes in ImageNet-21k without the overlapped classes with NUS-WIDE. We select 100 images for each class, so that the selected dataset contains 1.3M images which is the same level as ImageNet-1k (1.3M). The result of training on ImageNet-1k is shown on the first line of Table 8, and the second line shows the result of ImageNet-21k. With the number of available training classes becomes 15 times than before, the model mAP increases 6.9 points.

Train Dataset	Backbone	mAP(%)	F1(k=3)	F1(k=5)
ImageNet-1k	ViT-L-336	31.02	24.98	24.98
ImageNet-21k	ViT-L-336	37.92	39.82	40.39

Table 8. Comparisons of our method trained on the ImageNet-1k vs. ImageNet-21k dataset (filter the overlapped classes with NUS-WIDE) and tested on the NUS-WIDE dataset, with 336x336 resolution and ViT-L-336 backbone.

4.4.5 Experiments with Other VLP Models

Finally, we are also curious about how other VLP models perform under our method. We consider two examples BLIP [26] and SLIP [35]. They both have the contrastive loss similar to CLIP to ensure an alignment between the visual and textual features. In the second line of Table 9, the BLIP model with its ViT-L image encoder on 224×224 images shows a good result of 35.15%. SLIP in the third line shows similar performance. However, when we use a BLIP model that is fine-tuned on MS-COCO without the contrastive loss to ensure the alignment, the mAP quickly goes down to 2.52%. This strongly shows that the correlation between visual and textual embedding plays an important role in providing the performance boost, instead of the image or text encoder itself.

Image/Text Encoder	Backbone	Image Resolution	mAP(%)
BLIP	ViT-L(COCO)	384x384	2.52
BLIP	ViT-L	224x224	35.15
SLIP	ViT-L	224x224	34.15

Table 9. Applying other VLP models for alignment to our method on NUS-WIDE open-vocabulary multi-label classification task.

5. Conclusion

In this paper, we present a novel open-vocabulary multi-label classification framework called Aligned Dual modality ClaSsifier (ADDS). The framework is based on textual-visual alignment and leverages a novel Dual-Modal Decoder design and a Pyramid-Forwarding technique. Our method significantly outperforms all previous results and becomes the state-of-the-art method on open-vocabulary multi-label classification, single-to-multi label classification, and also conventional multi-label classification tasks.

References

- [1] Zeynep Akata, Florent Perronnin, Zaid Harchaoui, and Cordelia Schmid. Label-embedding for image classification. *IEEE transactions on pattern analysis and machine intelligence*, 38(7):1425–1438, 2015. [2](#), [7](#)
- [2] Emanuel Ben-Baruch, Tal Ridnik, Nadav Zamir, Asaf Noy, Itamar Friedman, Matan Protter, and Lihi Zelnik-Manor. Asymmetric loss for multi-label classification. *arXiv preprint arXiv:2009.14119*, 2020. [2](#), [6](#), [7](#)
- [3] Avi Ben-Cohen, Nadav Zamir, Emanuel Ben-Baruch, Itamar Friedman, and Lihi Zelnik-Manor. Semantic diversity learning for zero-shot multi-label classification. In *Proceedings of the IEEE/CVF International Conference on Computer Vision*, pages 640–650, 2021. [1](#), [2](#), [7](#)
- [4] Maria A Bravo, Sudhanshu Mittal, and Thomas Brox. Localized vision-language matching for open-vocabulary object detection. In *Pattern Recognition: 44th DAGM German Conference, DAGM GCPR 2022, Konstanz, Germany, September 27–30, 2022, Proceedings*, pages 393–408. Springer, 2022. [3](#)
- [5] Tianshui Chen, Muxin Xu, Xiaolu Hui, Hefeng Wu, and Liang Lin. Learning semantic-specific graph representation for multi-label image recognition. In *Proceedings of the IEEE/CVF international conference on computer vision*, pages 522–531, 2019. [2](#), [7](#)
- [6] Zhao-Min Chen, Xiu-Shen Wei, Peng Wang, and Yanwen Guo. Multi-label image recognition with graph convolutional networks. In *Proceedings of the IEEE/CVF conference on computer vision and pattern recognition*, pages 5177–5186, 2019. [7](#)
- [7] Tat-Seng Chua, Jinhui Tang, Richang Hong, Haojie Li, Zhiping Luo, and Yantao Zheng. Nus-wide: a real-world web image database from national university of singapore. In *Proceedings of the ACM international conference on image and video retrieval*, pages 1–9, 2009. [6](#)
- [8] Jia Deng, Wei Dong, Richard Socher, Li-Jia Li, Kai Li, and Li Fei-Fei. Imagenet: A large-scale hierarchical image

- database. In *2009 IEEE conference on computer vision and pattern recognition*, pages 248–255. Ieee, 2009. [1](#), [6](#)
- [9] Alexey Dosovitskiy, Lucas Beyer, Alexander Kolesnikov, Dirk Weissenborn, Xiaohua Zhai, Thomas Unterthiner, Mostafa Dehghani, Matthias Minderer, Georg Heigold, Sylvain Gelly, et al. An image is worth 16x16 words: Transformers for image recognition at scale. *arXiv preprint arXiv:2010.11929*, 2020. [3](#), [5](#), [6](#), [8](#)
- [10] Yu Du, Fangyun Wei, Zihe Zhang, Miaoqing Shi, Yue Gao, and Guoqi Li. Learning to prompt for open-vocabulary object detection with vision-language model. In *Proceedings of the IEEE/CVF Conference on Computer Vision and Pattern Recognition*, pages 14084–14093, 2022. [2](#)
- [11] Hironobu Fujiyoshi, Tsubasa Hirakawa, and Takayoshi Yamashita. Deep learning-based image recognition for autonomous driving. *IATSS research*, 43(4):244–252, 2019. [1](#)
- [12] Bin-Bin Gao and Hong-Yu Zhou. Learning to discover multi-class attentional regions for multi-label image recognition. *IEEE Transactions on Image Processing*, 30:5920–5932, 2021. [1](#), [2](#)
- [13] Mingfei Gao, Chen Xing, Juan Carlos Niebles, Junnan Li, Ran Xu, Wenhao Liu, and Caiming Xiong. Open vocabulary object detection with pseudo bounding-box labels. In *Computer Vision–ECCV 2022: 17th European Conference, Tel Aviv, Israel, October 23–27, 2022, Proceedings, Part X*, pages 266–282. Springer, 2022. [3](#)
- [14] Golnaz Ghiasi, Xiuye Gu, Yin Cui, and Tsung-Yi Lin. Open-vocabulary image segmentation. *arXiv preprint arXiv:2112.12143*, 2021. [2](#), [3](#)
- [15] Golnaz Ghiasi, Xiuye Gu, Yin Cui, and Tsung-Yi Lin. Scaling open-vocabulary image segmentation with image-level labels. In *Computer Vision–ECCV 2022: 17th European Conference, Tel Aviv, Israel, October 23–27, 2022, Proceedings, Part XXXVI*, pages 540–557. Springer, 2022. [3](#)
- [16] Xiuye Gu, Tsung-Yi Lin, Weicheng Kuo, and Yin Cui. Open-vocabulary object detection via vision and language knowledge distillation. *arXiv preprint arXiv:2104.13921*, 2021. [3](#)
- [17] Akshita Gupta, Sanath Narayan, Salman Khan, Fahad Shahbaz Khan, Ling Shao, and Joost van de Weijer. Generative multi-label zero-shot learning. *arXiv preprint arXiv:2101.11606*, 2021. [2](#), [7](#)
- [18] Dat Huynh and Ehsan Elhamifar. A shared multi-attention framework for multi-label zero-shot learning. In *Proceedings of the IEEE/CVF conference on computer vision and pattern recognition*, pages 8776–8786, 2020. [2](#), [7](#)
- [19] Andreas Kamilaris and Francesc X Prenafeta-Boldú. Deep learning in agriculture: A survey. *Computers and electronics in agriculture*, 147:70–90, 2018. [1](#)
- [20] Jin-Hwa Kim, Jaehyun Jun, and Byoung-Tak Zhang. Bilinear attention networks. *Advances in neural information processing systems*, 31, 2018. [2](#), [7](#)
- [21] Wonjae Kim, Bokyung Son, and Ildoo Kim. Vilt: Vision-and-language transformer without convolution or region supervision. In *International Conference on Machine Learning*, pages 5583–5594. PMLR, 2021. [3](#)

- [22] Diederik P Kingma and Jimmy Ba. Adam: A method for stochastic optimization. [arXiv preprint arXiv:1412.6980](#), 2014. [6](#)
- [23] Weicheng Kuo, Yin Cui, Xiuye Gu, AJ Piergiovanni, and Anelia Angelova. F-vm: Open-vocabulary object detection upon frozen vision and language models. [arXiv preprint arXiv:2209.15639](#), 2022. [3](#)
- [24] Chung-Wei Lee, Wei Fang, Chih-Kuan Yeh, and Yu-Chiang Frank Wang. Multi-label zero-shot learning with structured knowledge graphs. In [Proceedings of the IEEE conference on computer vision and pattern recognition](#), pages 1576–1585, 2018. [1](#)
- [25] Gen Li, Nan Duan, Yuejian Fang, Ming Gong, and Daxin Jiang. Unicoder-vl: A universal encoder for vision and language by cross-modal pre-training. In [Proceedings of the AAAI Conference on Artificial Intelligence](#), volume 34, pages 11336–11344, 2020. [3](#)
- [26] Junnan Li, Dongxu Li, Caiming Xiong, and Steven Hoi. Blip: Bootstrapping language-image pre-training for unified vision-language understanding and generation. [arXiv preprint arXiv:2201.12086](#), 2022. [3](#), [8](#)
- [27] Liunan Harold Li, Mark Yatskar, Da Yin, Cho-Jui Hsieh, and Kai-Wei Chang. Visualbert: A simple and performant baseline for vision and language. [arXiv preprint arXiv:1908.03557](#), 2019. [3](#)
- [28] Qing Li, Weidong Cai, Xiaogang Wang, Yun Zhou, David Dagan Feng, and Mei Chen. Medical image classification with convolutional neural network. In [2014 13th international conference on control automation robotics & vision \(ICARCV\)](#), pages 844–848. IEEE, 2014. [1](#)
- [29] Tsung-Yi Lin, Michael Maire, Serge Belongie, James Hays, Pietro Perona, Deva Ramanan, Piotr Dollár, and C Lawrence Zitnick. Microsoft coco: Common objects in context. In [European conference on computer vision](#), pages 740–755. Springer, 2014. [6](#)
- [30] Shilong Liu, Lei Zhang, Xiao Yang, Hang Su, and Jun Zhu. Query2label: A simple transformer way to multi-label classification. [arXiv preprint arXiv:2107.10834](#), 2021. [1](#), [2](#), [3](#), [6](#), [7](#)
- [31] Yongcheng Liu, Lu Sheng, Jing Shao, Junjie Yan, Shiming Xiang, and Chunhong Pan. Multi-label image classification via knowledge distillation from weakly-supervised detection. In [Proceedings of the 26th ACM international conference on Multimedia](#), pages 700–708, 2018. [7](#)
- [32] Jueqing Lu, Lan Du, Ming Liu, and Joanna Dipnall. Multi-label few/zero-shot learning with knowledge aggregated from multiple label graphs. [arXiv preprint arXiv:2010.07459](#), 2020. [1](#)
- [33] Chaofan Ma, Yuhuan Yang, Yanfeng Wang, Ya Zhang, and Weidi Xie. Open-vocabulary semantic segmentation with frozen vision-language models. [arXiv preprint arXiv:2210.15138](#), 2022. [3](#)
- [34] Tomas Mikolov, Kai Chen, Greg Corrado, and Jeffrey Dean. Efficient estimation of word representations in vector space. [arXiv preprint arXiv:1301.3781](#), 2013. [1](#)
- [35] Norman Mu, Alexander Kirillov, David Wagner, and Saining Xie. Slip: Self-supervision meets language-image pre-training. [arXiv preprint arXiv:2112.12750](#), 2021. [3](#), [8](#)
- [36] Sanath Narayan, Akshita Gupta, Salman Khan, Fahad Shahbaz Khan, Ling Shao, and Mubarak Shah. Discriminative region-based multi-label zero-shot learning. In [Proceedings of the IEEE/CVF International Conference on Computer Vision](#), pages 8731–8740, 2021. [2](#), [7](#)
- [37] Mohammad Norouzi, Tomas Mikolov, Samy Bengio, Yoram Singer, Jonathon Shlens, Andrea Frome, Greg S Corrado, and Jeffrey Dean. Zero-shot learning by convex combination of semantic embeddings. [arXiv preprint arXiv:1312.5650](#), 2013. [2](#), [7](#)
- [38] Alec Radford, Jong Wook Kim, Chris Hallacy, Aditya Ramesh, Gabriel Goh, Sandhini Agarwal, Girish Sastry, Amanda Askell, Pamela Mishkin, Jack Clark, et al. Learning transferable visual models from natural language supervision. In [International Conference on Machine Learning](#), pages 8748–8763. PMLR, 2021. [3](#), [6](#)
- [39] Ricardo Rendall, Ivan Castillo, Bo Lu, Brenda Colegrove, Michael Broadway, Leo H Chiang, and Marco S Reis. Image-based manufacturing analytics: Improving the accuracy of an industrial pellet classification system using deep neural networks. [Chemometrics and Intelligent Laboratory Systems](#), 180:26–35, 2018. [1](#)
- [40] Tal Ridnik, Emanuel Ben-Baruch, Asaf Noy, and Lihi Zelnik-Manor. Imagenet-21k pretraining for the masses. [arXiv preprint arXiv:2104.10972](#), 2021. [1](#), [6](#)
- [41] Tal Ridnik, Gilad Sharir, Avi Ben-Cohen, Emanuel Ben-Baruch, and Asaf Noy. Ml-decoder: Scalable and versatile classification head. [arXiv preprint arXiv:2111.12933](#), 2021. [1](#), [2](#), [3](#), [4](#), [6](#), [7](#), [8](#)
- [42] Min Shi, Yufei Tang, Xingquan Zhu, and Jianxun Liu. Multi-label graph convolutional network representation learning. [IEEE Transactions on Big Data](#), 2020. [2](#)
- [43] Zhouxia Wang, Tianshui Chen, Guanbin Li, Ruijia Xu, and Liang Lin. Multi-label image recognition by recurrently discovering attentional regions. In [Proceedings of the IEEE international conference on computer vision](#), pages 464–472, 2017. [1](#), [2](#)
- [44] Hao Yang, Joey Tianyi Zhou, Yu Zhang, Bin-Bin Gao, Jianxin Wu, and Jianfei Cai. Exploit bounding box annotations for multi-label object recognition. In [Proceedings of the IEEE Conference on Computer Vision and Pattern Recognition](#), pages 280–288, 2016. [1](#), [2](#)
- [45] Jinyu Yang, Jiali Duan, Son Tran, Yi Xu, Sampath Chanda, Liqun Chen, Belinda Zeng, Trishul Chilimbi, and Junzhou Huang. Vision-language pre-training with triple contrastive learning. In [Proceedings of the IEEE/CVF Conference on Computer Vision and Pattern Recognition](#), pages 15671–15680, 2022. [3](#)
- [46] Jin Ye, Junjun He, Xiaojiang Peng, Wenhao Wu, and Yu Qiao. Attention-driven dynamic graph convolutional network for multi-label image recognition. In [European conference on computer vision](#), pages 649–665. Springer, 2020. [2](#)
- [47] Renchun You, Zhiyao Guo, Lei Cui, Xiang Long, Yingze Bao, and Shilei Wen. Cross-modality attention with semantic graph embedding for multi-label classification. In [Proceedings of the AAAI conference on artificial intelligence](#), volume 34, pages 12709–12716, 2020. [2](#), [7](#)

[48] Alireza Zareian, Kevin Dela Rosa, Derek Hao Hu, and Shih-Fu Chang. Open-vocabulary object detection using captions. In Proceedings of the IEEE/CVF Conference on Computer Vision and Pattern Recognition, pages 14393–14402, 2021. [1, 3](#)

[49] Yang Zhang, Boqing Gong, and Mubarak Shah. Fast zero-shot image tagging. In 2016 IEEE Conference on Computer Vision and Pattern Recognition (CVPR), pages 5985–5994. IEEE, 2016. [2, 3, 7](#)